O-Glycan Analysis of Natural Human Neutrophil Gelatinase B Using a Combination of Normal Phase- HPLC and Online Tandem Mass Spectrometry: Implications for the Domain Organization of the Enzyme†

Taj S. Mattu,‡,⊥ Louise Royle,‡ Jim Langridge,§ Mark R. Wormald,‡ Philippe E. Van den Steen,|| Jo Van Damme,|| Ghislain Opdenakker,|| David J. Harvey,‡ Raymond A. Dwek,*,‡ and Pauline M. Rudd*,‡

Glycobiology Institute, Department of Biochemistry, University of Oxford, South Parks Road, Oxford, OX1 3QU, United Kingdom, Micromass UK Ltd., Floats Road, Wythenshawe, Manchester, M23 9LZ, United Kingdom, and Laboratory of Molecular Immunology, Rega Institute, University of Leuven, Minderbroederstraat 10, 3000 Leuven, Belgium

Received June 15, 2000

ABSTRACT: Gelatinase B is a matrix metalloproteinase (MMP-9) expressed under strict control by many cell types including neutrophils, monocytes, macrophages, and tumor cells. MMP-9 is a key mediator in the physiological maintenance of the extracellular matrix both in tissue remodeling and development, while uncontrolled enzyme activity contributes to pathologies such as cancer and inflammation. Neutrophils release MMP-9 from granules in response to IL-8 stimulation. Human MMP-9 has three potential N-linked glycosylation sites and contains a Ser/Pro/Thr rich domain, known as the type V collagen-like domain, which is expected to be heavily O-glycosylated. Indeed, approximately 85% of the total sugars on human neutrophil MMP-9 are O-linked. This paper presents the detailed analysis of picomole amounts of these O-glycans using a novel HPLC-based strategy for O-glycan analysis that provides linkage and arm specific information in addition to monosaccharide sequence. The initial structural assignments were confirmed using HPLC with online MS/MS fragmentation analysis. Twelve sugars were identified that contained from two to nine monosaccharide residues. Most of these contained type 2 core structures with Galβ1-4GlcNAc (*N*-acetyl lactosamine) extensions, with or without sialic acid or fucose. The O-glycans were modeled using the oligosaccharide structural database. On the basis of the structure of gelatinase A (MMP-2), a model of MMP-9 suggests that the type V collagen-like domain in gelatinase B is located on a loop remote from the active site. Fourteen potential O-glycosylation sites are multiply presented on this loop of 52 amino acids. Many of the O-glycans identified contain terminal galactose residues that may provide recognition epitopes. Importantly, heavy glycosylation of this loop region, absent in gelatinase A, has considerable implications for the domain organization of MMP-9.

Gelatinase B (MMP-9)[1] is a multidomain enzyme (Figure 1, panel a) and a member of the family of matrix metalloproteinases (MMPs; collagenases, stromelysins, matrilysin, gelatinases, and membrane-type metalloproteinases) that control the remodeling of the extracellular matrix (ECM) (*1*, *2*). The enzymes form a protease cascade in which the zymogen form of each is activated by a "cysteine switch" mechanism operated by proteolytic cleavage of the zymogen. This event is followed by a conformational change and a second proteolytic cleavage that removes the propeptide (*3*). MMP-9 is expressed in neutrophils, monocytes, macrophages, and tumor cells and is a key mediator in the physiological maintenance of the extracellular matrix both in tissue remodeling and development. The levels of active enzyme are under tight regulation, for example, by the tissue inhibitor of metalloproteases-1 (TIMP-1). Uncontrolled

† The work in the Oxford Glycobiology Institute (GBI) was supported by the Biotechnology and Biological Sciences Research Council/Department of Trade and Industry LINK scheme, the European Commission (Grant BIO4-CT95-0138), and Oxford GlycoSciences Ltd. The research conducted in the Rega Institute was supported by the National Fund for Scientific Research (FWO-Vlaanderen), the Geconcerteerde OnderzoeksActies, Belgium, and Fortis Insurances AB, Belgium. Philippe E. Van den Steen is a research assistant of the FWO.

* To whom correspondence should be addressed at The Glycobiology Institute, Department of Biochemistry, University of Oxford, South Parks Road, Oxford OX1 3QU, U.K. Fax: +44 1865 275216. Telephone: +44 1865 275340. E-mail: pmr@glycob.ox.ac.uk.

‡ University of Oxford.

§ Micromass UK Ltd.

|| University of Leuven.

⊥ Current address: Jefferson Center for Biomedical Research, Thomas Jefferson University, 700 East Butler Avenue, Doylestown, PA 18901.

[1] Abbreviations: 2-AB: 2-aminobenzamide; ABS: *Arthrobacter ureafaciens* sialidase, AMF: almond meal α-fucosidase; BTG: bovine testes β-galactosidase; CLF: *Charonia lampas* α-fucosidase; CV: collagen type V domain; ECM: extracellular matrix; ESI: electrospray ionisation; FN: fibronectin; Fuc (F): fucose; Gal: galactose; GalNAc: *N*-acetylgalactosamine; GlcNAc: *N*-acetylglucosamine; gu: glucose unit; H: hexose; HPLC: high performance liquid chromatography; IgA1: immunoglobulin A1; LC: liquid chromatography; LPS: lipopolysaccharide; MALDI: matrix assisted laser desorption/ionization; MMP: matrix metalloproteinase; MS: mass spectrometry; N: *N*-acetyl hexosamine; NDV: Newcastle disease virus sialidase; NGAL: neutrophil gelatinase B-associated lipocalin; NP: normal phase; SDS−PAGE: sodium dodecylsulphate polyacrylamide gel electrophoresis; OGS: Oxford GlycoSciences plc; PNGase-F: peptide *N*-glycosidase F; PTH: phenylthiohydantoins; Q-TOF: quadrupole time-of-flight; S: *N*-acetylneuraminic acid; SPG: *Streptococcus pneumoniae* β-galactosidase; SPH: *Streptococcus pneumoniae* β-*N*-acetyl hexosaminidase; TFA: trifluoroacetic acid; TOF: time-of-flight; Zn: zinc binding domain.

10.1021/bi001367j CCC: $19.00
Published on Web 12/02/2000

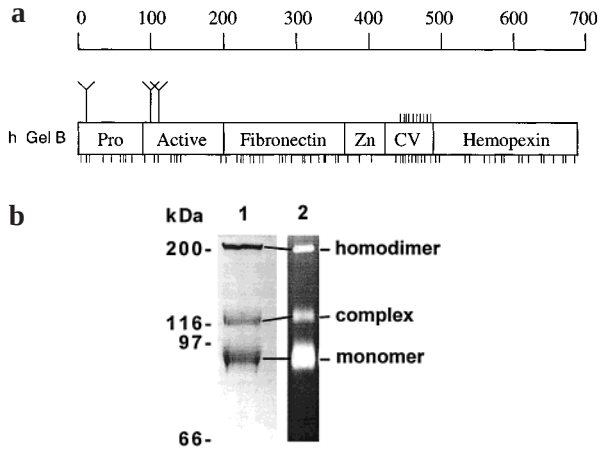

FIGURE 1: (a) Domain structure and glycosylation sites of gelatinase B. The scale at the top shows the number of amino acids in the proteins. Gelatinase B consists of seven domains, some of which are homologous with previously characterized domains in other proteins such as FN: fibronectin; Zn: zinc binding domain; CV: collagen type V domain and hemopexin. N-linked glycosylation sites are denoted by the symbol Y; potential sites of O-glycosylation (Ser and Thr residues) are denoted by the symbol |. (b) Natural gelatinase B from human neutrophils. Gelatinase B was purified to homogeneity and analyzed by protein staining with Coomassie blue (lane 1) and by gelatin zymography (lane 2). In both instances, a nonreducing SDS-containing polyacrylamide slab gel was used. A molecular mass standardization protein sample was processed in parallel, and the masses are indicated at the left. At the right, the 92-kDa gelatinase B monomer and the homodimer, as well as the heterodimer complex, are indicated. The latter consists of gelatinase B, covalently linked to neutrophil gelatinase B-associated lipocalin (NGAL).

enzyme activity contributes to pathologies such as cancer and inflammation and may play a role in rheumatoid arthritis and multiple sclerosis. In contrast to gelatinase A (MMP-2), which is constitutively secreted (e.g., from fibroblasts), neutrophil gelatinase B is stored in granules and is released only when the cells are stimulated to degranulate, for example, by IL-8 (*4*−*7*).

The amino acid sequence of human and mouse gelatinase B, as deduced from molecular cloning experiments (*8*, *9*), indicates that the molecule contains three N-linked glycosylation sequons close to the N-terminus at sequons Asn^{19}−Leu−Thr, Asn^{101}−Ile−Thr, and Asn^{108}−Tyr−Ser. The N-glycans from recombinant murine MMP-9, expressed in the yeast *Pichia pastoris* (*10*), and natural human neutrophil MMP-9 (*11*) have been sequenced. The N-glycans represent only about 15% of the total glycans attached to MMP-9. The remainder are O-linked glycans (*11*) that are most probably attached to a section of primary sequence, the type V collagen-like domain, which is located between residues 452 to 503 (Figure 1, panel a). This domain is rich in Pro (18 residues), Ser (2 residues), and Thr (12 residues) residues and is characteristic of a peptide region that contains clustered O-linked glycans, such as in mucins, the hinge region of IgA1 and in decay accelerating factor (*12*−*14*). Assuming the three N-linked sites are fully occupied, it can be estimated that human neutrophil gelatinase B contains approximately 17 O-glycans, suggesting that some are located at individual Ser or Thr sites outside the type V collagen-like domain (Figure 1, panel a).

Mucin type O-glycosylation is a common posttranslational modification. In the secretory pathway, O-glycans are attached to fully folded proteins, typically in the Golgi. The process is initiated by the transfer of an *N*-acetylgalactosamine residue to the hydroxyl group in a Ser or Thr side chain by one of the family of GalNAc transferase enzymes (*13*). Although O-glycans are often clustered in regions of primary sequence rich in Ser/Pro/Thr, isolated Ser or Thr residues may also be glycosylated. A number of functions are emerging for O-linked glycans (*14*). However, as compared with N-glycans (*15*), roles for O-glycosylation are less well established.

Potential functions for sugars can best be explored by viewing the glycoprotein as a whole, and this requires that structural data relating to the protein be complemented by data from glycan analysis. O-linked sugars have proved difficult to analyze, with the result that few data are available that enable proteins to be modeled with O-glycans attached. To address this problem, we have developed novel HPLC-based technology to provide a rapid, sensitive strategy for O-glycan analysis. Previously, we developed a combination of normal phase-HPLC, mass spectrometry, and exoglycosidase digestions to elucidate N-linked glycan structures (*11*, *16*−*20*). This technology has now been extended to analyze O-linked glycans (*12*). In this paper, we present the first application of the new strategy to the analysis of a natural glycoprotein containing large O-glycans.

The O-linked glycans from gelatinase B were released by optimized hydrazinolysis and fluorescently labeled with 2-aminobenzamide (2-AB). Structures were assigned from the elution positions of the glycans on NP-HPLC combined with the results of exoglycosidase digestions and electrospray ionization (ESI) fragmentation data (*21*).

The structures of 12 O-linked glycans attached to human neutrophil gelatinase B were elucidated and then modeled using the oligosaccharide database (*22*). This has given a more complete overview of MMP-9 by complementing protein and N-glycan structural data (*11*). Heavy glycosylation of the type V collagen-like domain could have considerable implications for the domain organization of MMP-9, and the clustered O-glycans may also function as recognition epitopes.

MATERIALS AND METHODS

Preparation and Analysis of Gelatinase B from Human Neutrophils. Human neutrophils were isolated from the buffy coats of blood donations (Red Cross, Antwerp, Belgium) as described (*23*). After 24 h stimulation of the samples with lipopolysaccharide (LPS) from *E. coli* (0111.B4; Difco Laboratories, Detroit, MI) (2 μg/mL) at 37 °C in serum-free Dulbecco's minimal essential medium, the cell supernatants were harvested, filtered, and purified by affinity chromatography on gelatin-Sepharose (*23*). The material was checked for purity by amino-terminal sequence analysis on an automated pulsed liquid sequencer (Applied Biosystems, model 477A). The phenylthiohydantoins (PTH) were identified by HPLC analysis on a PTH C18 5-μm column (Applied Biosystems PTH-analyzer model 120A). Gel analysis was as described earlier (*11*).

O-Glycan Release and Fluorescent Labeling. Neutrophil gelatinase B (60 μg) was dialyzed against 0.1% TFA and lyophilized. O-glycans were released via manual hydrazinolysis as described previously (*12*). Following paper chromatography, glycans were recovered from the origin by

elution with water. The nonreduced glycan pool was evaporated to dryness using a vacuum centrifuge and fluorescently labeled via a reductive amination reaction with 2-aminobenzamide (2-AB) using the Oxford GlycoSciences (OGS) Signal Labeling kit (*24*), and excess label was removed by ascending paper chromatography with acetonitrile.

Analysis of O-Glycans by Normal Phase-High Performance Liquid Chromatography (*HPLC*). Normal phase (NP) HPLC separations were performed using a GlycoSep-N chromatography column (4.6 × 250 mm; OGS) fitted to a Waters Alliance 2690 Separations module equipped with a Jasco FP-920 fluorescence detector (E_{ex} 330 nm, E_{em} 420 nm). The low salt buffer system of 50 mM ammonium formate buffer (pH 4.4) was used as described previously (*16*). Briefly, the linear gradient started at 80% acetonitrile and decreased to 42% over 152 min with a concomitant increase in the concentration of the ammonium formate buffer.

Simultaneous Exoglycosidase Sequencing of the Released Glycan Pool. Aliquots (~10 pmol) of the O-glycan pool were evaporated to dryness in a vacuum centrifuge. Ten microliters of standardized enzyme solutions was added, and the mixtures were incubated for 16−24 h at 37 °C in the manufacturer's (OGS) recommended buffers. Conditions for the individual enzymes in the arrays were as follows: *Arthrobacter ureafaciens* sialidase (EC 3.2.1.18, ABS): 1−2 U/mL; almond meal α-fucosidase (EC 3.2.1.111, AMF): 3 mU/mL; *Charonia lampas* α-fucosidase (EC 3.2.1.51, CLF; Oxford Glycobiology Institute): 10 U/mL with 1 mg/mL BSA; bovine testes β-galactosidase (EC 3.2.1.23, BTG): 1−2 U/mL; *Streptococcus pneumoniae* β-*N*-acetyl hexosaminidase (EC 3.2.1.30, SPH): 0.1 U/mL; Newcastle disease virus neuraminidase (Hitchner B1 strain: EC 3.2.1.18, NDV): 0.2 U/mL in 50 mM sodium acetate; substrate concentration 20 μM. Samples were purified from the exoglycosidases before HPLC analysis by passing through a microcentrifuge tube inset with a protein binding filter (Microspin 45 μm CN, Pro-Mem, R. B. Radley and Co Ltd., Shire Hill, Saffron Walden, Essex, UK). Glycans were recovered by washing the filter with 15 μL of 5% acetonitrile.

Microbore Liquid Chromatography Electrospray Tandem Mass Spectrometry of O-Glycans. A microbore NP-HPLC column (1 × 150 mm) was made using the stationary phase material from a GlycoSep N column (OGS). This was installed on a CapLC (Waters Corp., Milford, MA) module interfaced with a Q-TOF hybrid quadrupole time-of-flight mass spectrometer with electrospray ionization fitted with a Z-Spray ion source (Micromass UK Ltd., Wythenshawe, Manchester, UK). In this study, there was not sufficient material to allow optimization of the instrument settings for sensitivity. The fluorescently labeled O-glycans (70 pmol) released from human gelatinase B isolated from neutrophils were injected onto the microbore NP-HPLC column and chromatographed using a variant of the NP-HPLC conditions (*16*) as mentioned earlier. The conditions used for the microbore system included a more rapid gradient starting at 80% acetonitrile and decreasing to 50% over 60 min. This gradient segment was followed by an increase in ammonium formate buffer concentration to 100% over the next 10 min before re-equilibration to the starting conditions. The flow rate was 40 μL/min. No flow splitting was used, and all the chromatography effluent was injected into the Z-spray ion source. Data were collected at 16 points/Da using a mass range of 430 to 1500. Automatic MS to MS/MS switching was initiated when the signal rose above a threshold of 10. A fall in the intensity to below a threshold of 2 switched the scan back from MS/MS to MS mode. Initial conditions were source temperature 90 °C, cone voltage 31 V, ion energy 1.7 V, and the MS collision energy 4.0 V, mass range 430 to 1500. The scan duration was 1 s, and the interscan delay was 0.1 s. The settings for MS/MS were the same except that the scan range was from 50 to 1400, and the collision energy ranged from 17 to 21 V, depending on mass. For data evaluation, we relied on mass profiling of the initial mass survey (MS^1) for ions consistent with known carbohydrate compositions (including the 2-AB fluorescent tag). Only those ions with both *m*/*z* values and an isotopic distribution consistent with carbohydrates were evaluated. The MS/MS fragmentation of the ion clusters that did match the *m*/*z* and isotopic distribution of carbohydrates were then investigated to confirm the predicted structural assignments.

Molecular Modeling. Molecular modeling was performed on a Silicon Graphics Indigo 2 workstation using InsightII and Discover software (MSI Inc.). Figures were produced using the program Molscript (*25*). The molecular model of gelatinase B was based on the crystal structure of gelatinase A (*26*) obtained from the pdb database (*27*). The hemopexin domains were moved relative to the other domains to allow for the 56-residue insertion between the zinc binding domain and the hemopexin domain. No attempt was made to model the structure of the insertion. N- and O-glycan structures, chosen on the basis of the sequencing results, were generated using the database of glycosidic linkage conformations (*22*) and in vacuo energy minimization to relieve unfavorable steric interactions. The N-glycans were modeled onto the pro-peptide and active site domains. The O-glycans are only shown to give an idea of the relative sizes of the sugars to the protein domains.

RESULTS

Purification of Neutrophil Gelatinase B. Gelatinase B secreted by human peripheral blood neutrophils was purified by affinity chromatography on gelatin-Sepharose. From SDS−PAGE analysis (Figure 1, panel b), the sample was estimated to contain approximately 50% of monomeric gelatinase B, 35% of the dimeric form, and 15% of the heterodimer of gelatinase B with NGAL. Amino-terminal sequence analysis (after SDS−PAGE) returned sequences consistent with the full-length leukocyte gelatinase B (Leu−Val−Leu−Phe−Pro−Gly−Asp-) and gelatinase B truncated by two residues (Leu−Phe−Pro−Gly−Asp−Leu−Arg-). No contamination with either gelatinase A or the tissue inhibitor of metalloproteases was identified. The purified material was able to cleave gelatin and, using zymography, was shown to migrate at a relative molecular mass of 90−95 kDa. Both a homodimer of gelatinase B (~200 kDa) and a heterodimer of gelatinase B with NGAL (130 kDa) were also visualized by zymography, consistent with the literature (*28*). Following de-*N*-glycosylation with PNGase F treatment (data not shown), the appearance and size of the homo- and heterodimer decreased as well as the relative molecular mass of the monomer (*11*). The remaining heterogeneity of the de-*N*-glycosylated material was concluded to be a consequence of O-glycosylation, equivalent to an addition of >10 kDa to the predicted amino acid composition (76 kDa).

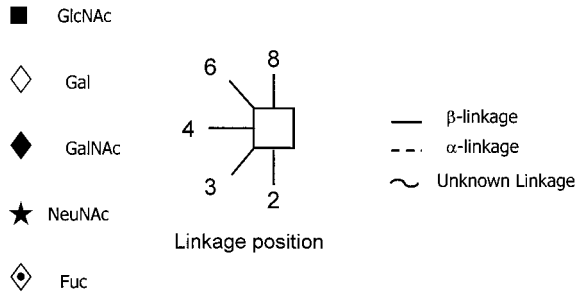

FIGURE 2: Nomenclature for the diagrammatic representation of oligosaccharides. Each monosaccharide is represented by a particular symbol, the shading of which has been chosen to represent substituents: for example, an open symbol means the sugar is not substituted, while the filled symbol indicates that the monosaccharide contains a *N*-acetyl group, or a dot indicates a deoxy sugar. Hence Gal is represented by an open diamond; GalNAc by a blackened diamond; and deoxy-galactose (fucose) by an open diamond with a dot inside. The linkage positions are represented by the angle of the line linking adjacent monosaccharides. As most sugars are linked via the C1 reducing end (except sialic acids which are linked via C2), this information is not represented in these diagrams. It is the position to which the reducing end of the sugar to the left attaches to the sugar on the right, which is represented by bond angle. A straight line indicates a beta-linkage, a dotted line indicates an alpha linkage. Where the exact monosaccharide is unknown (e.g., from mass spec data), an appropriately shaded symbol is used, e.g., an open hexagon for a hexose, and a filled hexagon for a HexNAc. Unknown linkages are represented by a wavy line. This simple visual representation of both sugars and linkages clearly conveys the structural information needed when working with complex glycan structures.

Analysis of Gelatinase B O-Glycans. HPLC Analysis of Released O-Glycan Pool. The O-glycans from neutrophil gelatinase B were released by manual hydrazinolysis at 60 °C for 4 h under conditions designed to minimize degradation (*11*). The reduced and re-*N*-acetylated glycan pool was fluorescently labeled with 2-AB and resolved by NP-HPLC (Figure 3, top panel). The nomenclature for describing the O-glycans pictorially is shown in Figure 2. Aliquots from the pool were then digested with exoglycosidases, singly and in arrays. The HPLC analyses of a selection of these digests are shown in Figure 3. The data indicated that neutrophil gelatinase B contains a series of O-glycans that vary in size from the neutral core 1 disaccharide (Galβ1-3GalNAc) to elongated structures modified with sialic acid and/or fucose (Table 1). The glycan structures were confirmed by comparing their elution positions with those of standard sugars and by the use of incremental values for particular monosaccharide additions (Royle, L., Rudd, P. M., and Dwek, R. A., manuscript in preparation).

Confirmation of HPLC-Based Assignments by Q-TOF Mass Spectrometry. All HPLC-based assignments were confirmed by mass spectrometry (Table 2). For example, the oligosaccharide eluting at 4.63 gu (Figure 3, top panel; Table 1) was shown to have a composition of H_2N_2S (see abbreviations) [observed monoisotopic mass of the $[M + H]^+$ ion, *m*/*z* 1160.6 (Table 2, peak 6)]. The presence of the Y ion fragment at *m*/*z* 795.5 (calculated, *m*/*z* 795.3) was consistent with a composition of a single hexose, HexNAc, and sialic acid attached to 2-AB (HNS-2AB). Other Y ion fragments at *m*/*z* 707.5 (HN_2-2AB), *m*/*z* 869.6 (H_2N_2-2AB), *m*/*z* 998.7 (HN_2S), and a B fragment ion of *m*/*z* 366.3 (HN) were all consistent with a galactosylated core 2 structure with

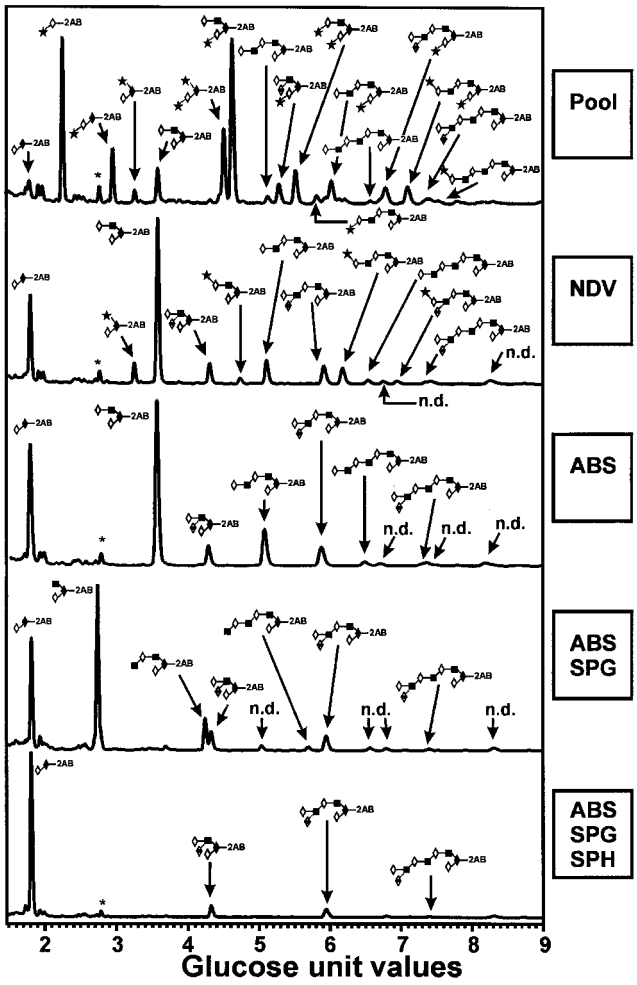

FIGURE 3: Exoglycosidase sequencing of neutrophil gelatinase B O-linked glycans monitored by NP-HPLC. Aliquots of the total 2-AB labeled O-glycan pool were incubated with different exoglycosidases, as shown in each panel. Following digestion, the products were analyzed by NP-HPLC, and the data (time *x*-axis) were linearized to the glucose unit scale on the *x* axis using a new computer program (Peak Time, E. Hart, unpublished data). The major peaks have been annotated. Structures were determined (Table 1) from the elution position of the peaks, measured in gu, relative to known standards (Royle et al., manuscript in preparation) and the specificity of the exoglycosidases used. Digestions were performed singularly, then in combination. The figures show only a selection of the digests performed. The enzymes used are indicated in the boxes on the right with abbreviations as follows: ABS: *Arthrobacter ureafaciens* sialidase; NDV: Newcastle disease virus sialidase; SPG: *Streptococcus pneumoniae* β-galactosidase; SPH: *Streptococcus pneumoniae* β-*N*-acetyl hexosaminidase.

a single sialic acid on the core 1 galactose. The nomenclature used for the description of the fragment ions is based upon that of Domon and Costello (*29*). When the sample was exposed to different exoglycosidases, this peak at 4.63 gu migrated to smaller gu values in a manner consistent with the structure proposed (Figure 3). Thus, treatment with Newcastle disease virus sialidase, which is unable to hydrolyze the α2-6 linkage, leads to a peak migrating at a gu value consistent with the nonsialylated galactosylated core 2 structure (3.57 gu). This peak was further degraded to one at 2.74 gu following combined treatment with the generic sialidase from *Arthrobacter ureafaciens* (ABS) and a galactosidase specific for the Galβ1-4 linkage from *Streptococcus pneumoniae* (SPG). The location of the sialic acid to the core

Table 1: Analysis of the O-Glycans from Human Neutrophil Gelatinase B[a]

glycan #	gu	glycan	enzyme digests: pool	NDVS	ABS	ABS, SPG	ABS, SPG, SPH
	1.42	nd		1.4	0.7	4.1	4.5
	1.73	nd		0.9	1.8	1.2	4.5
1	1.81	Galβ1-3GalNAc	2.3	16.9	23.0	21.0	63.4
2	2.29	NeuNAcα2-3Gal	18.4		0.5		
	2.74	GlcNAcβ1-6(Galα1-3)GalNAc		0.9	1.0	38.3	1.3
	2.78	nd	1.8	2.3	2.8	*	2.4
3	2.98	NeuNAcα2-3Galβ1-3GalNAc	6.4	0.6			
	3.29	NeuNAcα2-6(Galβ1-3)GalNAc	1.6	4.4			
4	3.57	Galβ1-4GlcNAcβ1-6(Galβ1-3)GalNAc	4.0	36.0	36.9	0.6	
	4.24	GlcNAcβ1-3/6Galβ1-4GlcNAcβ1-6(Galβ1-3)GalNAc				7.0	
	4.32	Galβ1-4(Fucα1-3)GlcNAcβ1-6(Galβ1-3)GalNAc		5.1	4.7	4.6	5.1
5	4.52	NeuNAcα2-6(NeuNAcα2-3Galβ1-3)GalNAc	9.6				
6	4.63	Galβ1-4GlcNAcβ1-6(NeuNAcα2-3Galα1-3)GalNAc	20.1				
	4.75	NeuNAcα2-6Galβ1-4GlcNAcβ1-6(Galβ1-3)GalNAc		1.3			
	5.12	Galβ1-4GlcNAcβ1-3/6Galβ1-4GlcNAcβ1-6(Galβ1-3)GalNAc	1.1	5.3	8.3		
7	5.28	Galβ1-4(Fucα1-3)GlcNAcβ1-6(NeuNAcα2-3Galβ1-3)GalNAc	2.7				
8	5.51	NeuNAcα2-3Galβ1-4GlcNAcβ1-6(NeuNAcα2-3Galβ1-3)GalNAc	4.1				
	5.93	Galβ1-4(Fucα1-3)GlcNAcβ1-3/6Galβ1-4GlcNAcβ1-6(Galβ1-3)GalNAc	0.7	4.2	4.4	3.5	3.9
	5.96	NeuNAcα2-6Galβ1-4GlcNAcβ1-6(NeuNAcα2-3Galβ1-3)GalNAc	3.1				
9	6.19	Galβ1-4GlcNAcβ1-6Galβ1-4GlcNAcβ1-6(NeuNAcα2-3Galβ1-3)GalNAc	0.7	3.8			
	6.55	Galβ1-4GlcNAcβ1-3/6Galβ1-4GlcNAcβ1-3/6Galβ1-4GlcNAcβ1-6(Galβ1-3)GalNAc		0.9	1.0	0.8	
10	6.77	Galβ1-4(Fucα1-3)GlcNAcβ1-3/6Galβ1-4GlcNAcβ1-6(NeuNAcα2-3Galβ1-3)GalNAc	2.7	0.6	0.7	0.6	0.6
11	7.08	NeuNAcα2-6Galβ1-4GlcNAcβ1-3/6Galβ1-4GlcNAcβ1-6(NeuNAcα2-3Galβ1-3)GalNAc	2.2				
	7.39	Galβ1-4(Fucα1-3)GlcNAcβ1-3/6Galβ1-4GlcNAcβ1-3/6Galβ1-4GlcNAcβ1-6 (Galβ1-3)GalNAc	1.1				
	7.51	NeuNAcα2-6Galβ1-4GlcNAcβ1-3/6Galβ1-4GlcNAcβ1-3/6Galβ1-4GlcNAcβ1-6 (Galβ1-3)GalNAc	1.1				
12	7.77	NeuNAcα2-6Galβ1-4(Fucα1-3)GlcNAcβ1-3/6Galβ1-4GlcNAcβ1-6 (NeuNAcα2-3Galβ1-3)GalNAc	2.2				
	8.15	nd	1.1				
13	8.27	Galβ1-4(Fucα1-3)GlcNAcβ1-3/6Galβ1-4GlcNAcβ1-3/6Galβ1-4GlcNAcβ1-6 (NeuNAcα2-3Galβ1-3)GalNAc	1.1				

[a] The table shows the peaks numbered as in Table 2 (column 1) gu values (column 2), assigned structures (column 3) and the percentages of the O-linked glycans B (column 4) released from human neutrophil gelatinase B. Percentages of the glycan populations (Figure 3) were calculated from the total integrated area, which includes all nondetermined (nd) structures. The enzymes used are at the top of each column (see list for definition of abbreviations). Asterisk (*): Peak obscured by adjacent large peak.

1 galactose, rather than the *N*-acetyl lactosamine galactose, was confirmed by incubation of the glycan pool with *Streptococcus* galactosidase. The NP-HPLC of the resultant products showed that the 4.63 gu peak was degraded to a peak consistent with the removal of one galactose (0.8 gu) (data not shown). Structures were assigned to the other glycans in a similar manner.

Neutrophil Gelatinase B Contains O-Glycans with a Type 2 Core. The preliminary structural assignments using the HPLC data did not allow the type of core structure to be assigned unambiguously. Many of the exoglycosidase array digestions suggested that the core structure of the larger O-glycans was type 1 even though the oligosaccharides co-eluted with core 2 standard glycans (isolated from bovine fetuin) on both NP- and RP-HPLC (data not shown) This ambiguity was due to the resistance of the core galactose in these larger structures to bovine testes β-galactosidase (data not shown). The MS/MS data distinguished between these two possibilities. Figure 4, panel a, shows the MS/MS collision-induced dissociation (CID) fragmentation spectra for the oligosaccharide eluting at 5.51 gu (Figure 3; Table 1, peak 8). The parent structure was identified as the doubly charged $[M + 2H]^{2+}$ ion with a *m*/*z* of 726.4 corresponding to a composition of $H_2N_2S_2$ (Table 3) (calculated *m*/*z* 726.3). Figure 4, panel b, shows the fragmentation pattern for the oligosaccharide, identified as a disialylated core 2 structure. The parent ions identified were almost exclusively hydrogen adducts, a consequence of the low cone voltage and the ammonium formate buffer system. This predominance of hydrogen adducts minimized the expected cross-ring fragmentation patterns associated with sodium adducts of carbohydrates (*30*) but simplified the interpretation of the resultant MS/MS data.

The presence of the $Y_{1\alpha}$ and $B_{3\alpha}$ (Figure 4) ions indicates that one sialic acid is on each galactose residue and that the structure includes the monosialylated core 1 moiety (*m*/*z* 795.5) with a HNS addition (*m*/*z* 657.4). The monosaccharide to which the HNS addition is linked (and hence which core structure is present) was determined by the identification of the $Y_{2\alpha/1\beta}$ peak at *m*/*z* 545.4, the composition of which is N_2 linked to 2-AB. The presence of the $Y_{2\alpha/1\beta}$ ion is consistent with the core 2 structure. Indeed, all the MS/MS CID fragmentation spectra recorded contained this particular ion. Thus, it was concluded that the larger oligosaccharides were core 2 structures with variations in fucose, sialic acid, and the number of *N*-acetyl lactosamine extensions. The ion at *m*/*z* 1160.7 ($Y_{3\alpha}$) could also have been produced by $Y_{2\beta}$; similarly *m*/*z* 998.7 ($Y_{2\alpha}$) could have been produced by $Y_{1\beta}$, and *m*/*z* 707.5 ($Y_{2\alpha/2\beta}$) could have been produced by a $Y_{1\beta/3\alpha}$ cleavage. However, the presence of the ion at *m*/*z* 366.3 could only have been produced by cleavage at $B_{3\alpha}/Y_{3\alpha}$, suggesting that the fragmentation pattern can be interpreted as indicated

Table 2: Analysis, by NP-HPLC-Q-TOF MSMS, of the O-Glycans from Human Neutrophil Gelatinase B

Peak #	Charge state[a]	Mass[b] Calculated	Mass[b] Observed	Composition[c] H	N	F	S	2-AB	Structure
1	[d][M+H]$^+$	504.2	n.d.	1	1	0	0	1	
2	[e][M+H]$^+$	592.2	592.4	1	0	0	1	1	
3	[M+H]$^+$	795.3	795.5	1	1	0	1	1	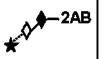
4	[M+H]$^+$	869.4	869.6	2	2	0	0	1	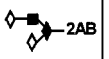
5	[M+H]$^+$	1086.4	1086.6	1	1	0	2	1	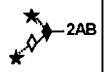
6	[M+H]$^+$	1160.4	1160.6	2	2	0	1	1	
7	[M+H]$^+$	1306.5	1306.7	2	2	1	1	1	
8	[M+2H]$^{2+}$	726.3	726.5	2	2	0	2	1	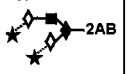
9	[M+2H]$^{2+}$	763.3	763.5	3	3	0	1	1	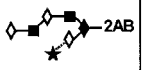
10	[M+2H]$^{2+}$	836.3	836.5	3	3	1	1	1	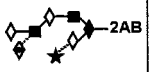
11	[M+2H]$^{2+}$	908.8	909.0	3	3	0	2	1	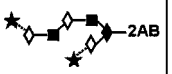
12	[M+2H]$^{2+}$	981.9	982.1	3	3	1	2	1	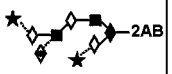
13	[M+2H]$^{2+}$	1018.9	1019.6	4	4	1	1	1	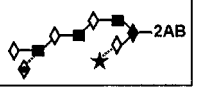

[a] Charge state of the predominant ion observed. [b] Monoisotopic mass of ion (2-AB derivative). [c] Monosaccharide composition, H = hexose, N = *N*-acetyl hexosamine, F = fucose, S = N-acetyl neuraminic acid, 2-AB = 2-aminobenzamide. [d] Predicted ion was not observed in MS survey due to coelution of $[M + 2X]^{2+}$ polymer material. [e] Predicted ion was observed in MS survey, but no MSMS data were recorded due to polymer material coeluting in this region.

in Table 2. It was noted that cleavage for $Y_{1\alpha}$ fragment formation appeared to be very favorable.

Analysis of Fucosylation. The addition of fucose to an *N*-acetyl lactosamine extension of N-linked glycans typically leads to an increase in retention of ~0.9 gu for addition via α1-3 linkage to GlcNAc or ~0.45 gu for addition via α1-2 linkage to galactose (*17*). The fucosylated derivative of the glycan eluting at 4.63 gu was identified by its mass increment (146 mass units) at 5.28 gu (Figure 3; Table 1), representing an incremental retention value of 0.65 gu. This fucosylated glycan oligosaccharide was also identified by mass spectrometry (peak 7, Table 2) and fragmented in a manner consistent with the structure proposed (data not shown). The discrepancy between the incremental retention values for fucose linked to α1-3GlcNAc on N- and O-linked glycans, highlights the need to determine specific incremental values for monosaccharide additions to O-glycans. The oligosaccharide eluting at 5.28 gu was resistant to streptococcal galactosidase and bovine epididymis fucosidase (α1-6 specificity; data not shown). However, a combination of SPG and almond meal fucosidase (α1-3,4 specificity) degraded the oligosaccharide to one eluting at 3.6 gu consistent with the loss of both a Galβ1-4 residue and a Fucα1-3 residue (*11*).

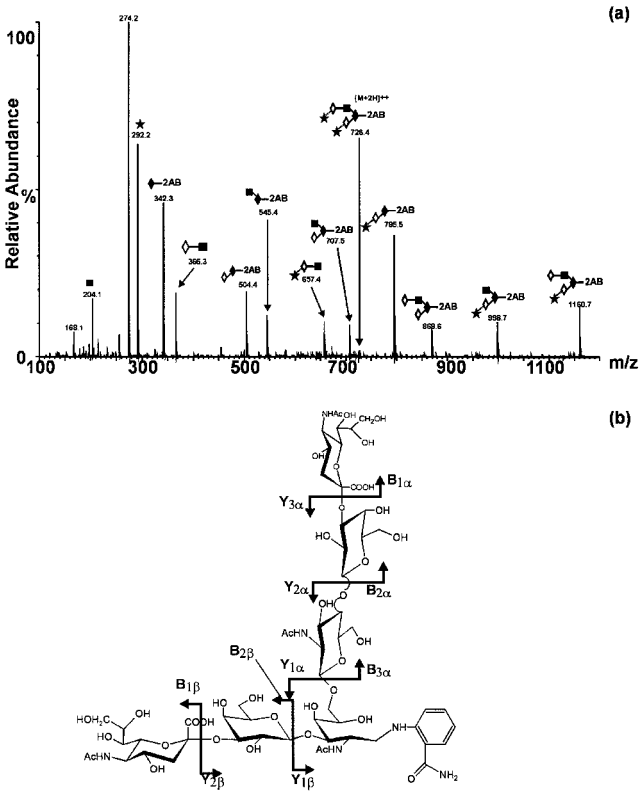

FIGURE 4: MS/MS characterization of the disialylated, galactosylated core 2 O-glycan following online HPLC. (a) MS/MS characterization of the glycans eluting at retention time 33 min, equivalent to 5.3 gu value. (b) Fragmentation scheme of the $[M + 2H]^{2+}$ ion at *m*/*z* 726.4. The nomenclature used for the fragmentation is based upon that of Domon and Costello (29) as listed in Table 3.

Table 3: Monosaccharide Composition, Masses, and MS^2 Fragmentation of Disialylated, Galactosylated Core 2 O-Glycan (Figure 4)

mass[a] calculated	mass[a] observed	composition[b] H	N	F	S	2-AB	fragment[c,d]
726.3	726.4	2	2	0	2	1	$[M + 2H]^{2+}$
1160.5	1160.7	2	2	0	1	1	$Y_{3\alpha}$
998.4	998.7	1	2	0	1	1	$Y_{2\alpha}$
869.4	869.6	2	2	0	0	1	$Y_{3\alpha/2\beta}$
795.3	795.5	1	1	0	1	1	$Y_{1\alpha}$
707.3	707.5	1	2	0	0	1	$Y_{2\alpha/2\beta}$
657.2	657.4	1	1	0	1	0	$B_{3\alpha}$
545.3	545.4	0	2	0	0	1	$Y_{2\alpha/1\beta}$
504.2	504.4	1	1	0	0	1	$Y_{1\alpha/2\beta}$
366.2	366.3	1	1	0	0	0	$B_{3\alpha}/Y_{3\alpha}$
342.2	342.3	0	1	0	0	1	$Y_{1\alpha/1\beta}$
292.1	292.2	0	0	0	1	0	$B_{1\alpha}$ and/or $B_{1\beta}$
274.1	274.2	0	0	0	1	0	$B_{1\beta}$ -H_2O and/or $B_{1\alpha}$ -H_2O
204.1	204.1	0	1	0	0	0	$B_{3\alpha}/Y_{2\alpha}$
	168.1						nd[e]

[a] Monoisotopic mass of ion (2-AB derivative). [b] Monosaccharide composition, H = hexose, N = *N*-acetyl hexosamine, F = fucose, S = *N*-acetyl neuraminic acid, 2-AB = 2-aminobenzamide. [c] Labeled according to pattern shown in Figure 4 and Domon and Costello (*29*). [d] All ions are singly charged with hydrogen, unless otherwise stated. [e] Not determined.

Assignment of O-Glycan Structures using a Combination of Predictive NP-HPLC, Exoglycosidase Digestions and MS

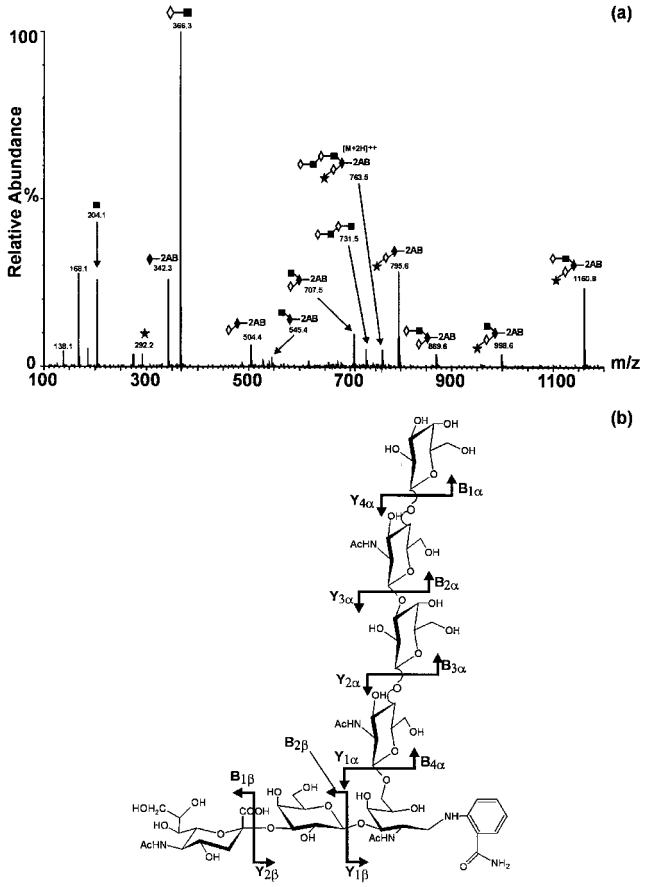

FIGURE 5: MS/MS characterization of the monosialylated, elongated core 2 O-glycan following on line HPLC. (a) MS/MS characterization of the glycans eluting at retention time 35 min, equivalent to 6.0 gu value. (b) Fragmentation scheme of the $[M + 2H]^{2+}$ ion at *m*/*z* 763.5, as listed in Table 4.

Fragmentation Data. By combining the predictive NP-HPLC, exoglycosidase digestions, and MS fragmentation data, structures could be assigned to the majority of the glycans. The elongated structures with either one (6.77 gu), or two (8.27 gu) additional *N*-acetyl lactosamine extension-(s) were also identified, together with analogues containing sialic acid and/or fucose, and their presence was confirmed by mass spectrometry. In the absence of a truly specific hexosaminidase, the linkage (β1-3/6) of the GlcNAc to Gal could not be determined, and the β1-3 isomer is shown throughout the paper.

Figure 5, panel a, shows the MS/MS spectrum of the *m*/*z* 763.5 $[M + 2H]^{2+}$ ion from the compound eluting at 6.19 gu (peak 9). The mass of the parent ion was consistent with the composition H_3N_3S (calculated *m*/*z* = 763.3, Table 4). The structure was predicted to be the galactosylated core 2 structure containing an additional *N*-acetyl lactosamine extension and one sialic acid. The fragmentation pattern of this oligosaccharide is shown in Figure 5, panel b. Because of the presence of the $Y_{1\alpha}$ ion (*m*/*z* 795.6) the position of attachment of the sialic acid was confirmed to be on the core 1 galactose residue. Had the sialic acid been attached via the Galβ1-4 residue, we would have expected to record the *m*/*z* 657.2 ion, analogous to $B_{3\alpha}$ fragment in Figure 4, panel b, Table 2. However, this ion was not observed. Consistent with the presence of a repeating *N*-acetyl lactosamine were the $B_{4\alpha}$ (H_2N_2, *m*/*z* 731.5) and $B_{2\alpha}$ (HN, *m*/*z* 366.3) ions.

Table 4: Monosaccharide Composition, Masses, and MS^2 Fragmentation of Monosialylated, Elongated Core 2 O-Glycan (Figure 5)

mass[a]		composition[b]					
calculated	observed	H	N	F	S	2-AB	fragment[c,d]
763.3	763.5	3	3	0	1	1	$[M + 2H]^{2+}$
1160.5	1160.8	2	2	0	1	1	$Y_{3\alpha}$
998.6	998.6	1	2	0	1	1	$Y_{2\alpha}$
869.4	869.6	2	2	0	0	1	$Y_{3\alpha/2\beta}$
795.3	795.6	1	1	0	1	1	$Y_{1\alpha}$
731.3	731.5	2	2	0	0	0	$B_{4\alpha}$
707.3	707.5	1	2	0	0	1	$Y_{2\alpha/2\beta}$
545.3	545.4	0	2	0	0	1	$Y_{2\alpha/1\beta}$
504.2	504.4	1	1	0	0	1	$Y_{1\alpha/2\beta}$
366.2	366.3	1	1	0	0	0	$B_{2\alpha}$ and/or $B_{4\alpha}/Y_{3\alpha}$
342.2	342.3	0	1	0	0	1	$Y_{1\alpha/1\beta}$
292.1	292.2	0	0	0	1	0	$B_{1\beta}$
274.1	274.2	0	0	0	1	0	$B_{1\beta}$ -H_2O
204.1	204.1	0	1	0	0	0	$B_{4\alpha}/Y_{2\alpha}$ and/or $B_{2\alpha}/Y_{4\alpha}$
	186.1						nd[e]
	168.1						nd
	138.10						nd

[a] Monoisotopic mass of ion (2-AB derivative). [b] Monosaccharide composition, H = hexose, N = *N*-acetyl hexosamine, F = fucose, S = *N*-acetyl neuraminic acid, 2-AB = 2-aminobenzamide. [c] Labeled according to pattern shown in Figure 5 and Domon and Costello (*29*). [d] All ions are singly charged with hydrogen, unless otherwise stated. [e] Not determined.

The mono-fucosylated derivative of this structure eluting at 6.7 gu was also identified. It gave a $[M + 2H]^{2+}$ ion at *m*/*z* 836.5. Its MS/MS CID fragmentation spectrum (Figure 6) produced the expected fragment ions (Table 5) of $B_{2\alpha}/Y_{4\alpha''}$ (*m*/*z* 366.3), the fucosylated derivative of this ion ($B_{2\alpha}$, *m*/*z* 512.3), as well as the nonfucosylated repeating *N*-acetyl-lactosamine $B_{4\alpha}/Y_{4\alpha''}$ (*m*/*z* 731.5) fragment and its fucosylated form ($B_{4\alpha}$, *m*/*z* 877.6). Intriguingly, fucose-containing ions were observed at *m*/*z* 1306.8, 1015.4, and 941.6 that were inconsistent with the proposed structure. They appeared to be products of internal monosaccharide(s) residue(s) loss. That is, although the external fucose-containing trisaccharide unit of Galβ1-4(Fucα1-3)GlcNAcβ1- is readily lost from the parent ion yielding the $Y_{3\alpha}$ fragment ion (*m*/*z* 1160.8), the ion at *m*/*z* 1306.8 had a mass that corresponded to a fucosylated derivative of this ion. Similarly, the ion at *m*/*z* 941.6 appeared to be a degradation product of this ion. These data could suggest that the position of fucose is on the core 2 GlcNAc residue. The presence of *m*/*z* 941.6 indicates that the fucose must have "migrated" across the molecule during the initial fragmentation which resulted in the loss of the first *N*-acetyl lactosamine unit. This type of internal residue loss has been reported before (*31*, *32*) for $[M + H]^+$-type ions but not for $[M + Na]^+$ ions. We explored this hypothesis and have confirmed with the aid of model compounds that, during CID fragmentation, protonated, but not sodium-cationized fucose-containing oligosaccharides fragment in such a manner that the fucose residue is able to migrate from one end of the molecule to the other. Specifically, the MS/MS spectra of the $[M + H]^+$ ions from the 2-AB derivatives of chromatographically homogeneous mono- and difucosylated analogues of the linear tetrasaccharide, Galβ1-3GlcNAcβ1-3Galβ1-4Glc, containing fucose on either or both of the nonreducing terminal galactose or GlcNAc residues, showed ions having the composition Fuc-$(Hex)_2$-2AB. These ions were absent from the MS/MS spectra of

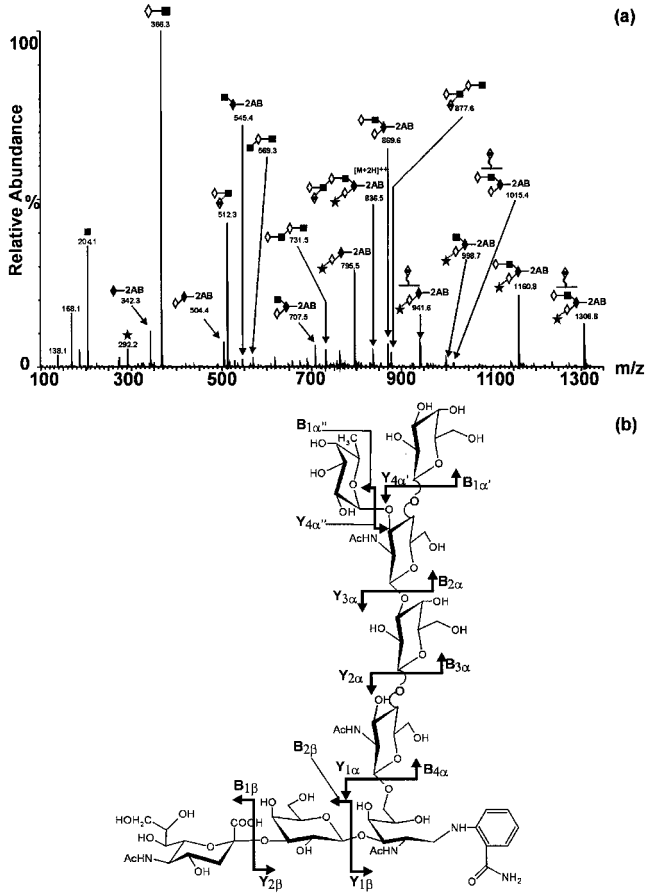

FIGURE 6: MS/MS characterization of the fucosylated, monosialylated, elongated core 2 O-glycan following online HPLC. (a) MS/MS characterization of the glycans eluting at retention time 39 min, equivalent to 6.7 gu value. (b) Fragmentation scheme of the $[M + 2H]^{2+}$ ion at *m/z* 836.5, as listed in Table 5.

Table 5: Monosaccharide Composition, Masses, and MS^2 Fragmentation of the Fucosylated, Monosialylated, Elongated Core 2 O-Glycan (Figure 6)

mass[a]		composition[b]					
calculated	observed	H	N	F	S	2-AB	fragment[c,d]
836.3	836.5	3	3	1	1	1	$[M + 2H]^{2+}$
763.3	763.5	3	3	0	1	1	$Y_{4\alpha''}{}^{++}$
1306.5	1306.8	2	2	1	1	1	$Y_{3\alpha}$ + fucose[f]
1160.5	1160.8	2	2	0	1	1	$Y_{3\alpha}$
1015.4	1015.4	2	2	1	0	1	$Y_{3\alpha/2\beta}$ + fucose[f]
998.4	998.7	1	2	0	1	1	$Y_{2\alpha/2\alpha}$
941.4	941.6	1	1	1	1	1	$Y_{1\alpha}$ + fucose[f]
877.3	877.6	2	2	1	0	0	$B_{4\alpha}$
869.4	869.6	2	2	0	0	1	$Y_{3\alpha/2\beta}$
795.3	795.5	1	1	0	1	1	$Y_{1\alpha}$
731.3	731.5	2	2	0	0	0	$B_{4\alpha}/Y_{4\alpha''}$
707.3	707.5	1	2	0	0	1	$Y_{2\alpha/2\beta}$
569.2	569.3	1	2	0	0	0	$B_{4\alpha}/Y_{4\alpha''/4\alpha'}$
545.3	545.4	0	2	0	0	1	$Y_{2\alpha/1\beta}$
512.2	512.3	1	1	1	0	0	$B_{2\alpha}$
504.2	504.4	1	1	0	0	1	$Y_{1\alpha/2\beta}$
366.2	366.3	1	1	0	0	0	$B_{2\alpha}/Y_{4\alpha''}$
342.2	342.3	0	1	0	0	1	$Y_{1\alpha/1\beta}$
292.1	292.2	0	0	0	1	0	$B_{1\beta}$
274.1	274.2	0	0	0	1	0	$B_{1\beta}$ -H_2O
204.1	204.1	0	1	0	0	0	$B_{2\alpha}/Y_{4\alpha'/4\alpha''}$ and/or $B_{4\alpha}/Y_{2\alpha}$
138.1	138.1						nd[e]

[a] Monoisotopic mass of ion (2-AB derivative). [b] Monosaccharide composition, H = hexose, N = *N*-acetyl hexosamine, F = fucose, S = *N*-acetyl neuraminic acid, 2-AB = 2-aminobenzamide. [c] Labeled according to pattern shown in Figure 6 and Domon and Costello (*29*). [d] All ions are singly charged with hydrogen, unless otherwise stated. [e] Not determined. [f] Rearrangement fragment ion, see text.

the corresponding $[M + Na]^+$ ions. Thus, during fragmentation of the $[M + H]^+$ ions, fucose must have migrated from the nonreducing-terminal residues to the reducing terminal hexose residues that were labeled with the 2-AB reagent (manuscript in preparation).

NP-HPLC-Q-TOF MSMS Analysis. Online NP-HPLC-MS/MS analysis allowed further identification of larger structures, confirmed the presence of the core 2 structure, and provided additional evidence for the location of the fucose residues. Reevaluating the NP-HPLC data with the aid of the MS and MS/MS data, allowed many more incremental values to be confirmed. This procedure, in turn, enabled the structures of the compounds producing some of the minor peaks to be predicted, although there was insufficient material to confirm the assignments. For example, a difucosylated core 2 structure of probable composition $H_3N_3F_2S$ was predicted for the peak labeled "nd" on the panel showing the NDV digest (Figure 3, ~6.85 gu).

MS and MS/MS data were collected using the automated facility since no online fluorescence detector compatible with the instrumentation was available. Some O-glycans (each representing no more than 2% of the total) were not present in sufficient quantities to be identified from the limited amount of sample available. The data that was collected and analyzed indicated that all the major glycans were selected for MS/MS analysis. Table 2 shows the composition and structure of all the oligosaccharides identified by NP-HPLC-Q-TOF MS/MS analysis.

DISCUSSION

In a previous study, the structures of the N-linked and the most abundant O-linked oligosaccharides in natural gelatinase B from neutrophils were identified (*11*). Approximately 85% of the sugars attached to human neutrophil gelatinase B are O-linked structures, most of which are presumably located in the type V collagen-like domain where there are 14 potential O-glycosylation sites in a stretch of 52 amino acids. As the quantities of natural glycoproteins are often limited, technology for detailed analysis of low levels of oligosaccharides remains a technical challenge. Here we developed and used novel technology to define all the O-linked oligosaccharides from gelatinase B, including the less abundant ones. Twelve sugars were identified that contained from two to nine monosaccharide residues. Most of these contained type 2 core structures with Galβ1-4GlcNAc (*N*-acetyl-lactosamine) extensions, with or without sialic acid or fucose.

Molecular Model of Gelatinase B and Potential Roles for the O-Glycans. A molecular model of gelatinase B, based on the crystal structure of gelatinase A, is shown in Figure 7. Gelatinase B contains an extra 56-residue domain not present in gelatinase A. This has been called the type V collagen-like domain because of the sequence homology with the α2 chain of collagen type V (*8*). However, the gelatinase B sequence does not have extensive GXX repeats; indeed very few of the collagen glycine residues are conserved, and instead it contains multiple threonine and serine residues.

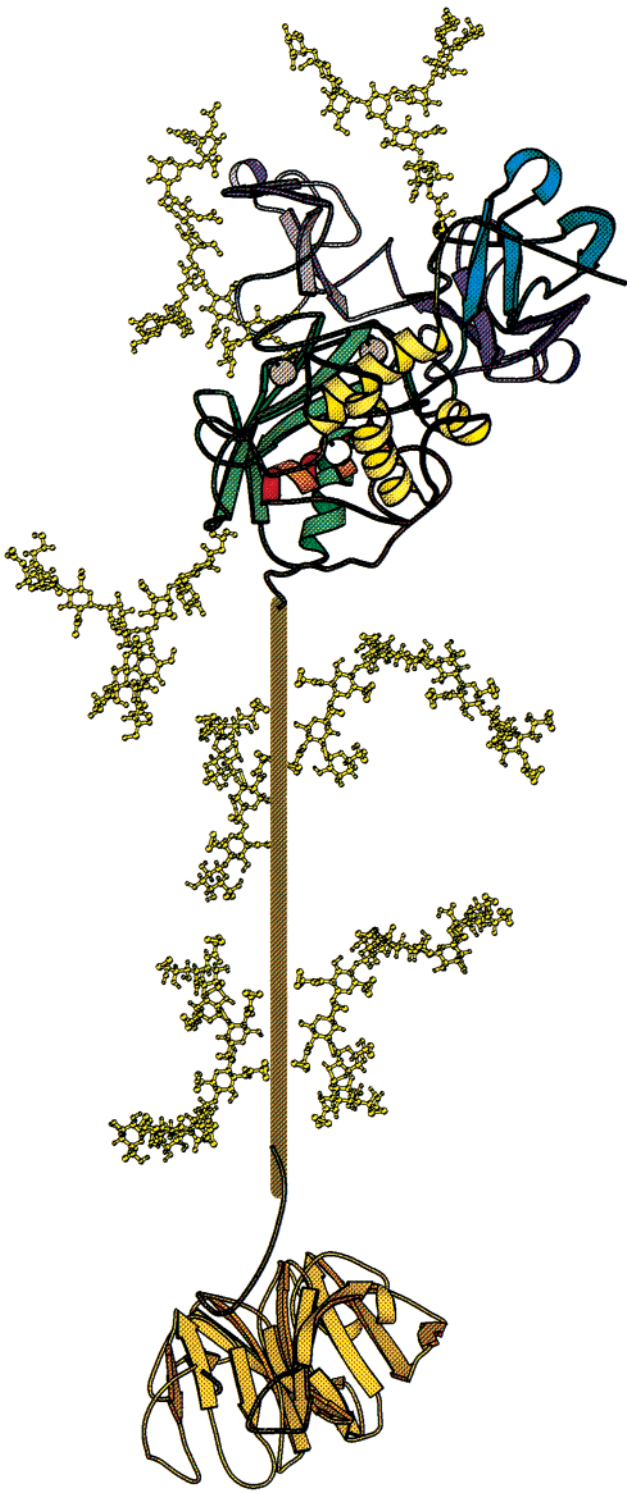

FIGURE 7: Molecular model of gelatinase B based on the crystal structure of gelantinase A (*26*). Yellow, pro peptide domain; green, active site domain; blue, fibronectin domains; red, zinc binding domain; orange, hemopexin domain. In the crystal structure of gelatinase A, the hemopexin domain is packed against the zinc binding domain with a disordered link between the two. Gelatinase B contains an additional domain between the zinc binding domain and the hemopexin domain not present in gelatinase A. This makes the quaternary organization of these domains in gelatinase B very uncertain (see Discussion). The additional 56-residue domain present in gelatinase B is represented by a solid bar. This contains 14 possible O-glycosylation sites. Four O-glycans (structures 6, 10, 11, and gu 7.51; see Tables 1 and 2) are shown for scale. Gelatinase B also contains three N-linked glycosylation sites, all of which are shown as occupied (A2G2F2 at site 19 in the pro-peptide domain and A2G2F1S2 at site 101 and A2G2F1S1 at site 108 in the active site domain). A2: biantennary; G2: digalactosylated; F1: core fucosylated; F2: core and outer arm fucosylated; S1: monosialylated; S2: disialylated.

The homology with collagen is mostly based on the high proline content of both sequences. Thus, the type V collagen-like domain in gelatinase B is very unlikely to have any structural homology with type V collagen. This region is hydrophilic, and extensive O-glycosylation of a peptide is known to result in chain extension and increased rigidity (*33*). The O-glycans found on the type V collagen-like domain are relatively large (see Figure 7) and could be expected to have a significant steric effect. The type V collagen-like domain may, therefore, act as an extended spacer between the zinc binding domain and the hemopexin domain. This has significant implications for the domain organization of gelatinase B. In the crystal structure of gelatinase A, the hemopexin domain is linked to the zinc binding domain by a short, disordered loop, but the domain still makes extensive crystallographic contacts. The presence of an extended, O-glycosylated spacer is likely to result in the hemopexin domain being separated from the N-terminal domains (as suggested in Figure 7).

The function of the O-linked sugars is not yet known, but, in common with other O-glycosylated protein domains, such as those in decay accelerating factor (*34*), IgA1 (*12*), and the LDL (*35*) and VLDL receptors (*36*), they would be expected to contribute to the stability of the enzyme and protect against proteolytic cleavage, in addition to any structural role in causing backbone conformational changes. This may be a critical function since gelatinase B is released from granules at inflammatory sites where proteases, including those that activate progelatinase B, are abundant.

The possible role of this domain is intriguing. Consideration of the molecular model indicates that the O-glycan laden domain will provide the molecule with a potential recognition site in which the sugars are multiply presented. This may allow gelatinase B to bind effectively to lectins, for example, galectins that recognize terminal galactose. Approximately 50% of the sugars contain terminal galactose. Such an interaction has been observed for the hinge glycans of IgA1 and IgD (*37*, *38*), which contain Galβ1,3-GalNAc-rich O-linked glycans and bind the IgD receptor on human T-cells. In common with the fibronectin domain, the O-glycans may also locate gelatinase B to specific regions of the extracellular matrix without compromising its enzyme activity thus retaining the enzyme in situ where it might engage more efficiently in specific, localized degradation of connective tissue. This could prevent uncontrolled action and negative side effects when gelatinase B is released from neutrophil granules. Interestingly, MMP-9 and MMP-2 cleave galectin 3 (*39*), a galactose binding lectin that might be expected to bind the O-glycans on MMP-9. Such possibilities remain to be explored.

Future Technical Development. An important aspect of this study has been the development of novel technology to provide a detailed structural analysis of picomoles of O-glycans released from this natural MMP which is available only in limited amounts. This paper contains the first application of an HPLC-based strategy for O-glycan analysis that provides linkage and arm-specific information in addition to monosaccharide sequence. The structural assignments, made on the basis of HPLC elution positions expressed in glucose units (gu) by comparison with the elution positions of a standard dextran ladder, were confirmed using online MS/MS fragmentation analysis. A comparison of the gu

values obtained from the standard NP-HPLC sequencing column and the one used for the LC-MS/MS study show that the changes in the gradient and column diameter have minimal effect upon the resolution of the oligosaccharides (data not shown). Thus, a narrow-bore liquid chromatography system interfaced with a Q-TOF mass spectrometer affords a powerful new methodology for the elucidation of oligosaccharide structure, especially when it is combined with digestions using exoglycosidase arrays. This technology now allows femtomoles of sugars to be comprehensively analyzed for composition, structure and, in combination with exoglycosidase arrays, linkage. In this paper, we have reported how interfacing the chromatographic separation of fluorescently labeled O-glycans directly with a hybrid quadrupole orthogonal time-of-flight (Q-TOF) mass spectrometer has allowed the analysis of O-glycans to confirm structures and to provide a repertoire of new standards on which to base HPLC-based structural assignments for the future.

Although the current repertoire of specific exoglycosidases requires extending to cover more of the linkages specific to O-glycans, our expanding database of the chromatographic behavior of O-linked sugars on NP- and RP-HPLC and the corresponding database of oligosaccharide spectrometry fragmentation patterns is generating a powerful comprehensive oligosaccharide analysis technology. The aim is to make O-glycan analysis a routine operation so that the roles for O-glycans on natural proteins, such as human neutrophil gelatinase B, can be more readily explored.

ACKNOWLEDGMENT

P.M.R. thanks H.C.L. for her constant inspiration.

REFERENCES

1. Woessner, J. F., Jr. (1991) *FASEB J. 5*, 2145−2154.
2. Collier I. E., and Goldberg, G. I. (1998) *Handbook of Proteolytic Enzymes* (Barret, A. J., Rawlings, N. D., and Woessner, J. F., Ed.) pp 1205−1210, Academic Press, New York.
3. Van Wart, H. E., and Birkedal-Hansen, H. (1990) *Proc. Natl. Acad. Sci. U.S.A. 87*, 5578−5582.
4. Opdenakker, G., Masure, S., Proost, P., Billiau, A., and Van Damme, J. (1991) *FEBS Lett. 284*, 73−78.
5. Opdenakker, G., Masure, S., Grillet, B., and Van Damme, J. (1991) *Lymphokine Cytokine Res. 10*, 317−324.
6. Gijbels, K., Masure, S., Carton, H., and Opdenakker, G. (1992) *J. Neuroimmunol. 41*, 29−34.
7. Cuzner, M. L., and Opdenakker, G. (1999) *J. Neuroimmunol. 94*, 1−14.
8. Wilhelm, S. M., Collier, I. E., Marmer, B. L., Eisen, A. Z., Grant, G. A., and Goldberg, G. I. (1989) *J. Biol. Chem. 264*, 17213−17221.
9. Masure, S., Nys, G., Fiten, P., Van Damme, J., and Opdenakker, G. (1993) *Eur. J. Biochem. 218*, 129−141.
10. Van den Steen, P., Rudd, P. M., Proost, P., Martens, E., Paemen, L., Küster, B., Van Damme, J., Dwek, R. A., and Opdenakker, G. (1998) *Biochim. Biophys. Acta 1425*, 587−598.
11. Rudd, P. M., Mattu, T. S., Masure, S., Bratt, T., Van den Steen, P. E., Wormald, M. R., Küster, B., Harvey, D. J., Borregaard, N., Van Damme, J., Dwek, R. A., and Opdenakker, G. (1999) *Biochemistry 38*, 13937−13950.
12. Mattu, T. S., Pleass, R. J., Willis, A. C., Kilian, M., Wormald, M. R., Lellouch, A. C., Rudd, P. M., Woof, J. M., and Dwek, R. A. (1998) *J. Biol. Chem. 273*, 2260−2272.
13. Clausen, H., and Bennett, E. P. (1996) *Glycobiology 6*, 635−646.
14. Van den Steen, P., Rudd, P. M., Dwek, R. A., and Opdenakker, G. (1998) *Crit. Rev. Biochem. Mol. Biol. 33*, 151−208.
15. Rudd, P. M., and Dwek, R. A. (1997) *Curr. Opinion Biotech. 8*, 488−497.
16. Guile, G. R., Rudd, P. M., Wing, D. R., Prime, S. B., and Dwek, R. A. (1996) *Anal. Biochem. 240*, 210−226.
17. Guile, G. R., Harvey, D. J., O'Donnell, N., Powell, A. K., Hunter, A. P., Zamze, S., Fernandes, D. L., Dwek, R. A., and Wing, D. R. (1998) *Eur. J. Biochem. 258*, 623−656.
18. Rudd, P. M., Morgan, B. P., Wormald, M. R., Harvey, D. J., Van den Berg, C. W., Davis, S. J., Ferguson, M. A. J., and Dwek, R. A. (1997) *J. Biol. Chem. 272*, 7229−7244.
19. Chen, Y. J., Wing, D. R., Guile, G. R., Dwek, R. A., Harvey, D. J., and Zamze, S. (1998) *Eur. J. Biochem. 251*, 691−703.
20. Zamze, S., Harvey, D. J., Chen, Y. J., Guile, G. R., Dwek, R. A., and Wing, D. R. (1998) *Eur. J. Biochem. 258*, 243−270.
21. Abian, J., Oosterkamp, A. J., and Gelpi, E. (1999) *J. Mass Spectrom. 34*, 244−254.
22. Petrescu, A. J., Petrescu, S. M., Dwek, R. A., and Wormald, M. R. (1999) *Glycobiology 9*, 343−352.
23. Masure, S., Proost, P., Van Damme, J. and Opdenakker, G. (1991) *Eur. J. Biochem. 198*, 391−398.
24. Bigge, J. C., Patel, T. P., Bruce, J. A., Goulding, P. N., Charles, S. M., and Parekh, R. B. (1995) *Anal. Biochem. 230*, 229−238.
25. Kraulis, P. J. (1991) *J. Appl. Crystallogr. 24*, 946−950.
26. Morgunova, E., Tuuttila, A., Bergmann, U., Isupov, M., Lindqvist, Y., Schneider, G., and Tryggvason, K. (1999) *Science 284*, 1667−1670.
27. Berman, H. M., Westbrook, J., Feng, Z., Gilliland, G., Bhat. T. N., Weissig, H., Shindyalov, I. N., and Bourne, P. E. (2000) *Nucleic Acids Res. 28*, 235−242.
28. Kjeldsen, L., Bjerrum, O. W., Askaa, J., and Borregaard, N. (1992) *Biochem. J. 287*, 603−610.
29. Domon, B., and Costello, C. E. (1988) *Glycoconjugate J. 5*, 397−409.
30. Orlando, R., Bush, C. A., Fenselau, C. (1990) *Biomed. Environ. Mass Spectrom. 19*, 747−754.
31. Kovácik, V., Hirsch, J., Kovácik, P., Heerma, W., Thomas-Oates, J. E., and Haverkamp, J. (1995) *J. Mass Spectrom. 30*, 949−958.
32. Brüll, L. P., Kovácik, V., Thomas-Oates, J. E., Heerma, W., and Haverkamp, J. (1998) *Rapid Comm. Mass Spectrom. 12*, 1520−1532.
33. Gerken, T. A., Butenhof, K. J., and Shogren, R. (1989) *Biochemistry 28*, 5536−5543.
34. Kuttner-Kondo, L., Medof, M. E., Brodbeck, W., and Shoham, M. (1996) *Protein Eng. 9*, 1143−1149.
35. Kingsley, D. M., Kozarsky, K. F., Hobbie, L., and Krieger, M. (1986) *Cell 44*, 749−759.
36. Magrane, J., Reina, M., Pagan, R., Luna, A., Casaroli-Marano, R. P., Angelin, B., Gafvels, M., and Vilaro, S. (1999) *J. Lipid Res. 39*, 2172−2181.
37. Rudd, P. M., Fortune, F. M., Patel, T., Parekh, R. B., Dwek, R. A., Lehner, T. (1994) *Immunology 83*, 99−106.
38. Swenson, C., Patel, T., Parekh, R. B., Lakshmi Tamma, S. M., Coico, R. F., Thorbecke, G. J., and Amin, A. R. (1998) *Eur. J. Immunol. 28*, 2366−2372.
39. Ochieng, J., Green, B., Evans, S., James, O., and Warfield, P. (1998) *Biochim. Biophys. Acta 1379*, 97−106.

BI001367J